What Determines Inhomogeneous Linewidths in Semiconductor Microcavities?

D. M. Whittaker

Toshiba Cambridge Research Centre, 260 Cambridge Science Park, Milton Road, Cambridge CB4 4WE, United Kingdom

(Received 8 August 1997; revised manuscript received 1 December 1997)

Microcavity inhomogeneous linewidths are calculated numerically using a microscopic two dimensional model of the polariton interaction with quantum well disorder. The calculations show that in most structures the linewidths are determined by disorder scattering between polariton and exciton states. This is because motional narrowing effectively removes the contribution due to multiple scattering between polariton states. [S0031-9007(98)06159-6]

PACS numbers: 78.20.Bh, 71.35.Cc, 71.36.+c, 78.40.Pg

Recent experimental results [1] have shown the importance of motional narrowing in semiconductor microcavities. In a microcavity, the fundamental optical excitations are polaritons, arising from the coupling of a confined cavity photon mode to exciton states in quantum wells within the cavity. The spectral features associated with the polariton are broadened, both homogeneously due to the finite lifetime of the cavity photon, and inhomogeneously due to the interaction with disorder in the quantum wells. Motional narrowing occurs because the polaritons, being part photon, have very long wavelengths compared with those typical for excitons. The inhomogeneous broadening is therefore substantially reduced by averaging over a large area of the much shorter length scale disorder potential. It should be emphasized that the present usage of the term "motional narrowing" differs significantly from its meaning in spin systems, where it refers to the slowing down, by scattering, of a relaxation process [2].

The important physical parameters which determine the inhomogeneous linewidths are the dispersions of the exciton and photon, the strength of their interaction, and the statistical properties of the disorder. A good approximation is to treat each dispersion as parabolic, the finite photon mass of $M_l \sim 3 \times 10^{-5} m_e$ being a consequence of the effects of cavity confinement [3]. The exciton-photon coupling leads to the formation of two polariton branches, separated at resonance by the vacuum Rabi splitting, $\hbar\Omega \sim 5$ meV, which provides a measure of the strength of the interaction. Finally, the quantum well disorder potential is characterized by its amplitude V_0, of order a few meV, and a correlation length $l_c \sim 100$ Å.

The treatment of motional narrowing in Ref. [1] assumed the weak disorder limit, $V_0 \ll \hbar\Omega$, in which only scattering between low momentum polariton states on the same branch is allowed. It was then possible to use a simple scaling argument to predict the variation of the linewidths with detuning. However, it has since been shown [4] that the scaling argument predicts the actual value of the inhomogeneous linewidth, at resonance, to be $\Gamma_{2D} \sim V_0^2 E_c^{-1}$, where $E_c = \hbar^2/2M_l l_c^2$. For physically reasonable parameters, Γ_{2D} is extremely small, $\sim 10^{-4}$ meV, compared to the experimental inhomogeneous linewidths of about 0.3 meV. This disparity clearly indicates that the assumption of weak disorder underlying the scaling treatment is not correct for the sample of Ref. [1].

The main aim of this Letter is to demonstrate that, as well as the polariton multiple scattering processes leading to Γ_{2D}, there is a contribution to the linewidth due to disorder scattering between polariton and higher momentum exciton states. Such scattering is not included in the scaling treatment, since it assumes the polariton dispersion is perfectly parabolic, while in fact the two branches decouple at large wave vectors. The more realistic calculation described here uses a numerical simulation of a polariton in the presence of the disorder, which automatically includes both types of scattering. For present day structures, polariton to exciton scattering dominates the small polariton multiple scattering contribution. In this regime, the numerical results agree very well with a simpler model, similar to that proposed by Houdré *et al.* [5], in which the exciton is treated as an energetically broadened but spatially homogeneous oscillator. However, in higher quality samples, where $V_0 < \hbar\Omega/2$, scattering of polaritons into exciton states would become energetically impossible, and only the small polariton multiple scattering contribution would remain.

The model used here is physically similar to the one dimensional treatment of Savona *et al.* [6]. However, motional narrowing in one dimension is significantly less important than in two, because averaging over a 1D strip samples much less of the variation of the potential than an average over a 2D area of equivalent size. This difference can be seen very clearly by calculating the contribution of polariton multiple scattering to the linewidth in 1D, $\Gamma_{1D} \sim V_0^{4/3} E_c^{-1/3}$. For the same parameters that gave $\Gamma_{2D} \sim 10^{-4}$ meV, $\Gamma_{1D} \sim 10^{-1}$ meV, 3 orders of magnitude greater, and far more comparable to the experimental linewidths. This comparison suggests that such 1D calculations are not adequate to describe the balance between polariton multiple scattering and polariton to exciton scattering in real structures.

The numerical treatment is based on a two level model of the polariton, in which a discrete cavity mode couples to the exciton ground state. The exciton interacts with the

quantum well disorder potential, so in-plane momentum is not conserved. The model thus consists of coupled two dimensional partial differential equations describing the in-plane motion of both the exciton and cavity photon. This model contains a number of approximations, most notably the omission of excited exciton states and the lack of a proper treatment of the effects of the magnetic field applied in the experiments. These approximations restrict the possibilities for precise comparisons with experiment, but the good general agreement which is obtained suggests that the essential physics is included.

The Hamiltonian for the model system takes the form

$$H = \begin{pmatrix} -\frac{\hbar^2}{2M_l}\nabla^2 + \delta - i\gamma & \hbar\Omega/2 \\ \hbar\Omega/2 & -\frac{\hbar^2}{2M_e}\nabla^2 + V(\mathbf{r}) \end{pmatrix}. \quad (1)$$

In addition to the photon mass M_l, and the vacuum Rabi splitting, $\hbar\Omega$, discussed above, M_e is the exciton mass, δ the detuning of the cavity photon relative to the exciton, and γ the photon homogeneous width (due to escape through the mirrors). The quantum well disorder, $V(\mathbf{r})$, is a Gaussian stochastic potential, constructed in the Fourier domain, following the method described by Glutsch *et al.* [7]. Its amplitude, V_0, is defined as the width at half maximum of the potential probability distribution.

The inhomogeneously broadened spectra are calculated from the photon Green's function

$$G_k(t) = -i\langle\mu_k|e^{-iHt/\hbar}|\mu_k\rangle\theta(t), \quad (2)$$

where $|\mu_k\rangle$ represents a state of the system (not an eigenstate) consisting of a plane wave cavity photon with in-plane wave vector k and no exciton. All the results given in this Letter are for normal incidence, corresponding to $k = 0$. The Green's function describes how a photon which enters the cavity is scattered out of its initial plane wave state by interactions with the disordered exciton. The plotted spectra are actually the photon spectral functions, obtained by Fourier transforming the Green's function to give $\tilde{G}_k(\omega)$ and extracting the imaginary part. They correspond to what would be seen in an absorption measurement, but for well resolved features the linewidths should be the same in reflectivity experiments.

The Green's function is obtained using an approach similar to that of Glutsch *et al.* [7]. Starting from an initial state $|\psi(0)\rangle = |\mu_k\rangle$, the wave function $|\psi(t)\rangle$ is calculated by numerically solving the time dependent Schrödinger equation using the Hamiltonian Eq. (1). From the solution at each time t, $G_k(t)$ is found by evaluating $\langle\mu_k|\psi(t)\rangle = \langle\mu_k|e^{-iHt/\hbar}|\mu_k\rangle$. The calculation is carried out on a two dimensional spatial grid, using a standard alternating direction Crank-Nicholson algorithm [8]. The main difficulty is the need to use a grid which is fine enough to reveal the correlated structure of the potential, on a length scale $l_c \sim 100$ Å, yet large enough to avoid significant size quantization for the low mass photon states. The present numerical results are for a $2^{11} \times 2^{11}$ grid with spacing 100 Å, giving photon quantization energies $\sim$0.05 meV, considerably smaller than typical calculated linewidths of $\sim$0.3 meV.

Figure 1 shows spectra calculated for a realistic set of parameters: $M_l = 3 \times 10^{-5} m_e$, $M_e = 0.5 m_e$, $\hbar\Omega = 5$ meV, $V_0 = 3.5$ meV, and $l_c = 100$ Å. For clarity, the photon homogeneous linewidth, γ, has been set to zero. The spectra display the variations in intensity typical of an anticrossing between two states, only one of which, the photon, has intrinsic strength. Close to resonance, where the polariton branches are equal mixtures of photon and exciton, the two peaks have similar integrated strength. Further away from resonance, the more photonlike peak is strong, while the other, predominantly exciton, is weak. The figure also shows the bare exciton spectrum, which is asymmetrically broadened due to the finite exciton mass [9,10].

In Fig. 2, the linewidths measured from the spectra are plotted as a function of detuning. The asymmetry between the linewidths of the two branches at zero detuning is very apparent: the upper branch has a width of $\sim$1 meV, and the lower branch 0.25 meV. When a realistic photon homogeneous broadening of $\gamma = 1.25$ meV is included in the calculation, the widths become 1.4 and 0.6 meV, respectively, close to the experimental values of $\sim$1.5 and 0.75 meV found in Ref. [1]. However, because of the lack of a proper treatment of the magnetic field used in the experiments, this agreement can be regarded as only suggestive.

The solid lines in Figs. 1 and 2 show the results of a simpler model, which provides an excellent fit to the numerical data. In this model, the full exciton Green's function $\tilde{G}^e_{kk'}(\omega)$ is approximated by its diagonal part

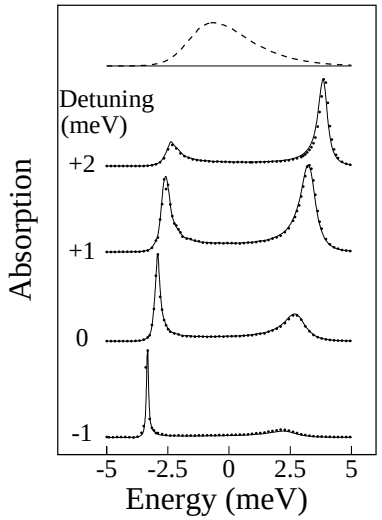

FIG. 1. Numerical absorption spectra (dots) at various values of the detuning δ. The dashed curve shows the bare exciton line shape. The solid lines are the predictions of the coupled oscillator model (see text).

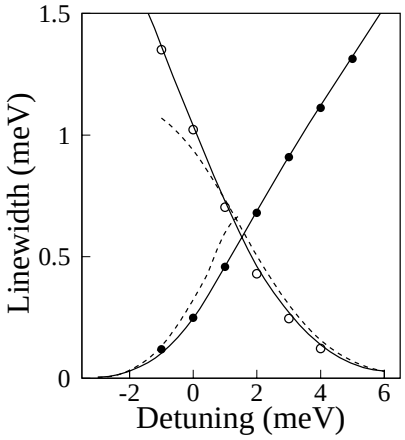

FIG. 2. Numerical linewidths as a function of detuning, δ, for upper (open symbols) and lower (filled symbols) polaritons. The solid lines are the predictions of the coupled oscillator model, the dashed lines those of the absorption model.

$\delta_{kk'}\tilde{G}^e_k(\omega)$. With k thus conserved, the polariton problem simplifies to a pair of coupled oscillators, which is easily solved to obtain the polariton Green's function

$$\tilde{G}_k(\omega) = \frac{1}{\hbar\omega + i\gamma - \delta_k - (\hbar\Omega/2)^2\,\tilde{G}^e_k(\omega)}, \qquad (3)$$

where $\delta_k = \delta + \hbar^2k^2/(2M_l)$ is the detuning for wave vector k. The bare exciton Green's functions $\tilde{G}^e_k(\omega)$ are calculated using the same type of numerical simulation as for the full polariton. However approximate expressions for the finite mass exciton spectral function, by Glutsch and Bechstedt [10], could be used for large exciton masses.

Equation (3) excludes polariton multiple scattering, since the polariton always has a definite wave vector k. However, polariton to exciton scattering processes are included, because the exciton Green's function $\tilde{G}^e_k(\omega)$ takes care of the scattering between exciton states. It has a finite imaginary self-energy determining the rate at which excitons scatter out of the state with wave vector k. The good fit to the numerical data which is obtained indicates that the contribution of polariton multiple scattering is negligible for these parameters, as is suggested by the estimate of Γ_{2D} given above.

An approximate expression for the polariton linewidths can be found by examining Eq. (3). For sufficiently small broadening, the polariton line shape approximates to a Lorentzian, with full width Γ dependent on the imaginary part of the denominator at the polariton energy, ω_p, according to

$$\Gamma = 2|c_l|^2[\gamma - (\hbar\Omega/2)^2\,\mathrm{Im}\{\tilde{G}^e_k(\omega_p)\}], \qquad (4)$$

where $|c_l|^2$ is the photon fraction of the polariton. This approximation is shown as the dashed lines in Fig. 2. For large photon fractions, when the polaritons are resonant with the tails of the exciton line (see Fig. 1), the approximate expression agrees fairly well with the exact curve. However, when $|c_l|^2$ becomes small, Eq. (4) predicts $\Gamma \to 0$, while the true value tends to the exciton linewidth. Equation (4) can be understood more physically by noting that the second term describes homogeneous broadening of the polariton due to the loss of photons in the cavity by absorption into exciton states—it is proportional to the photon fraction and the exciton absorption strength $-\mathrm{Im}\{\tilde{G}^e_k(\omega_p)\}$. This is to be be expected for states in the tail of the exciton line, which are too weak to require a strong coupling treatment, and thus act simply as a source of absorption in the cavity.

In the coupled oscillator model, the difference between the widths of the two polariton branches is a consequence of the asymmetry of the exciton lineshape, which is, in turn, a result of the finite exciton mass. On the low energy side of the line, there is an exponential cutoff, reflecting the distribution of minima in the disorder potential, while on the high energy side the strength falls off more slowly, as $\sim\omega^{-2}$, determined by the perturbation of high momentum plane wave states by the potential [11]. This explanation for the asymmetry is thus similar in essence to the suggestion by Savona *et al.* [6] that the larger upper branch width is caused by scattering of polaritons into higher momentum exciton states.

The coupled oscillator model can be shown to be a generalization of the phenomenological treatment of a spatially homogeneous but Gaussian broadened exciton, introduced by Houdré *et al.* [5]. The only significant technical difference is that the Gaussian exciton line shape is replaced by an asymmetic function because of the finite exciton mass. More importantly, the present work provides a justification for this treatment starting from a microscopic model of disorder, and emphasizes that it succeeds because motional narrowing effectively eliminates the polariton multiple scattering contribution to the linewidth.

The most intriguing feature of the Gaussian oscillator model, discussed by Savona and Weisbuch [12], is the prediction that the disorder contribution to the linewidth should disappear in high quality structures when polariton to exciton scattering becomes impossible. In terms of the absorption picture, this happens when the polariton states are so far into the tails of the exciton line that no absorption occurs. The present calculations support this prediction, as shown in Fig. 3, where numerical and coupled oscillator model linewidths are plotted as a function of disorder strength, V_0. As in Ref. [12], the lower branch width rapidly becomes very small when $V_0 < \hbar\Omega/2$. The effect is much less pronounced for the upper branch, because of the longer tail on the high energy side of the finite mass exciton line shape.

The numerical data in Figs. 1–3 are very well explained by the coupled oscillator model, which includes only polariton to exciton scattering. It is not possible in the calculations to resolve directly the small polariton multiple scattering term, Γ_{2D}, even for $V_0 \ll \hbar\Omega/2$, when it should be the only contribution to the linewidth. However,

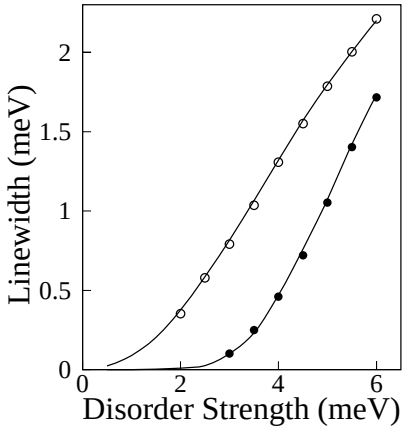

FIG. 3. Numerical linewidths as a function of disorder strength, V_0, for upper (open symbols) and lower (filled symbols) polaritons. The solid lines are the predictions of the coupled oscillator model.

indirect evidence for the existence of polariton multiple scattering can be obtained by using nonphysical parameters which make it more important. As an example, Fig. 4(a) shows the dependence on the photon mass, M_l, of the numerically simulated linewidths at resonance. The oscillator model predicts that the linewidths of the two branches should be equal, as the calculation is for infinite exciton mass, and independent of M_l. For the real $M_l = 3 \times 10^{-5} m_e$, the linewidths are indeed equal. However, when M_l is significantly increased a difference appears, which is clearly due to polariton multiple scattering, as it grows in proportion to Γ_{2D}, plotted as the dashed curve in the figure.

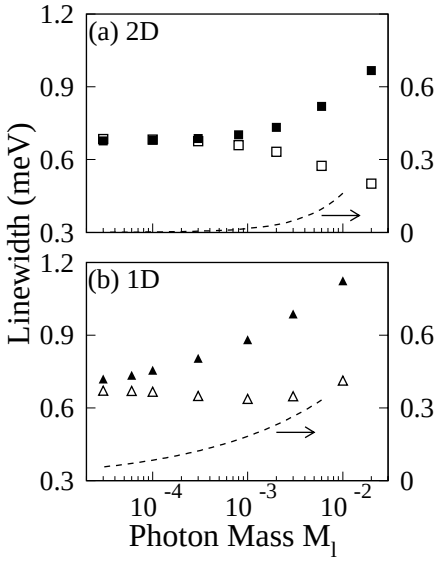

FIG. 4. Numerical linewidths as a function of photon mass, M_l, for upper (open symbols) and lower (filled symbols) polaritons in (a) two dimensions and (b) one dimension, with $M_e \to \infty$. Also shown (dashed lines and right hand scale) are the polariton multiple scattering expressions, Γ_{2D} and Γ_{1D} [13], discussed in the text.

Figure 4(b) shows similar data for a one dimensional system. Again, the difference between the upper and lower branch widths grows, for small M_l, in proportion to Γ_{1D}. However, even for the real $M_l = 3 \times 10^{-5} m_e$, there is a measurable difference in linewidths, some 0.05 meV. This result emphasizes the significant differences between the scattering processes which occur in 1D and 2D systems.

To summarize, the main conclusion of this Letter is that, in present day structures, a treatment of a spatially homogeneous exciton with a broadened line shape is adequate to understand experimental microcavity linewidths. Such a treatment corresponds to a model which includes only polariton to exciton scattering processes, omitting the effect of polariton multiple scattering on the linewidth. The justification for this model is that motional narrowing, due to the small polariton effective mass, renders the polariton multiple scattering contribution negligible. Thus, though it does not directly determine the experimental widths, as was suggested in Ref. [1], motional narrowing plays an essential role in explaining the reduced linewidths observed close to resonance.

I thank C. L. Foden, M. S. Skolnick, and J. J. Baumberg for many helpful discussions of this work.

[1] D. M. Whittaker, P. Kinsler, T. A. Fisher, M. S. Skolnick, A. Armitage, A. M. Afshar, M. D. Sturge, and J. S. Roberts, Phys. Rev. Lett. **77**, 4792 (1996).
[2] See, e.g., A. Abragam, in *The Principles of Nuclear Magnetism* (Clarendon, Oxford, 1961), p. 446.
[3] R. Houdré, C. Weisbuch, R. P. Stanley, U. Oesterle, P. Pellandini, and M. Ilegems, Phys. Rev. Lett. **73**, 2043 (1994).
[4] V. M. Agranovich, G. C. La Rocca, and F. Bassani (private communication).
[5] R. Houdré, R. P. Stanley, and M. Ilegems, Phys. Rev. A **53**, 2711 (1996).
[6] V. Savona, C. Piermarocchi, A. Quattropani, F. Tassone, and P. Schwendimann, Phys. Rev. Lett. **78**, 4470 (1997).
[7] S. Glutsch, D. S. Chemla, and F. Bechstedt, Phys. Rev. B **54**, 11 592 (1996).
[8] W. H. Press, S. A. Teukolsky, W. T. Vetterling, and B. P. Flannery, in *Numerical Recipes in Fortran* (Cambridge University Press, Cambridge, England, 1992), 2nd ed., pp. 838–848.
[9] R. F. Schnabel, R. Zimmermann, D. Bimberg, H. Nickel, R. Lösch, and W. Schlapp, Phys. Rev. B **46**, 9873 (1992).
[10] S. Glutsch and F. Bechstedt, Phys. Rev. B **50**, 7733 (1994).
[11] Al. L. Efros, C. Wetzel, and J. M. Worlock, Nuovo Cimento Soc. Ital. Fis. **17D**, 1447 (1995).
[12] V. Savona and C. Weisbuch, Phys. Rev. B **54**, 10 835 (1996).
[13] The plotted widths are actually $\Gamma_{2D}/2$ and $\Gamma_{1D}/4$, which fit better to calculations of the bare exciton linewidths in the strong motional narrowing limit.